Modeling Wireless Channel Fading

William Turin, Rittwik Jana,
AT&T Labs-Research
180 Park Avenue
Florham Park, NJ 07932

Carol Martin, Jack Winters
AT&T Labs-Research
200 Laurel Avenue S.
Middletown, NJ 07748

Abstract—**In this paper, we compare measured fading data with the popular Rayleigh model. Our results show that this model does not agree with the experimental data. As an alternative, we approximate the experimental data using autoregressive moving average (ARMA) models. To validate the models, we compare several characteristics of fading obtained analytically, by simulation, and from measured data.**

I. Introduction

Many papers and books are devoted to modeling fading communication channels. Common feature of the models is that they all have memory. The most popular model describes fading as a complex Gaussian process ([1], [2], [3]). In this paper, we investigate the validity of this model on the basis of experimental data ([6]). The measured data used in this study was obtained from field tests conducted to characterize the mobile multiple-input multiple-output (MIMO) radio channel. The MIMO test system consisted of a 4-branch base station receiver with rooftop antennas and 4 transmitters at the mobile with antennas mounted on a laptop computer. The base station rooftop and laptop antenna arrays used dual-polarized antennas with slant $\pm 45°$ polarization. For this study we used the measurements of the complex channel from one of the transmit antennas at the mobile to one of the base station antennas.

The field tests were conducted using a 30 kHz bandwidth, with bit and frame synchronous orthogonal sequences transmitted from each of the 4 transmitters at the mobile. Real-time baseband signal processing at the base station performed timing recovery and symbol synchronization, and calculated and recorded the complex channel measurements every 300 μsec. [1]

Extensive drive tests plus pedestrian and indoor tests were conducted at 1900 MHz from a typical cellular base station site located in a suburban environment. Data was collected along several drive routes including routes in a residential area and on a highway, with vehicle speeds of 30 and 65 mph, and downrange distances between 2 to 5 miles. Pedestrian tests were also conducted by walking with the terminal at several locations and placing it inside a house. Further details on the test system and measurements are presented in [6]. We have performed an additional filtering of the data to remove high frequency noise.

We compare theoretical models with measured data for two different cases: mobile moving in residential area (case "R") and highway (case "H"). In case R, vehicle moves at 30 mph while in case H it moves at 65 mph. Our results show that that estimated autocorrelation function of fading process, level crossing rate and mean fade duration differ from that of the theoretical Rayleigh model. As an alternative, we considered modeling of fading using autoregressive moving average (ARMA) models. These models are popular in many applications and are used as a major tool for systems identification. [4], [8] ARMA models allow us to approximate second order statistics of a process with high degree of accuracy. On the other hand, we can take advantage of the rich theory of fitting ARMA to experimental data. However, since ARMA models are linear and represent a special case of Markov processes, it might require to use high-order models to approximate accurately the experimental data. A more economical description can be obtained using more general nonlinear state-space models which are equivalent to the hidden Markov models [12], [11]. In this paper, we consider modeling of the fade inphase component. The quadrature component has a similar model.

Our paper is organized as follows. In section 2 we compare the most popular model for the Rayleigh fading ([2]) with measured data. In section 3 we consider various models for the fading envelope. We conclude in section 4.

II. Clarke's Model

Let $x(t)$ be a low-pass equivalent of the transmitted signal with the inphase component $x_I(t) = Re\{x(t)\}$ and quadrature component $x_Q(t) = Im\{x(t)\}$. Consider a frequency-nonselective fading channel with the additive noise $n(t)$. This channel can be modeled as ([7], p. 716)

$$y(t) = c(t)x(t) + n(t) \tag{1}$$

where $y(t)$ is the received signal and fading is modeled by the complex random process $c(t)$. Different models are based on different assumptions about $c(t)$ and $n(t)$.

The most popular models assumes that $c(t)$ and $n(t)$ are complex stationary zero-mean Gaussian processes with independent and identically distributed real and imaginary parts. The PDF of a sequence $\mathbf{c}_k = (c(t_1), c(t_2), ..., c(t_k))$ has the form

$$f(\mathbf{c}_k) = (2\pi)^{-k}|\mathbf{D}|exp(-0.5\mathbf{c}_k\mathbf{D}\mathbf{c}_k^H) \tag{2}$$

where $|\mathbf{D}|$ denotes determinant of $\mathbf{D}$, $\mathbf{c}_k^H$ denotes the conjugate transpose of $\mathbf{c}_k$, and $\mathbf{D}^{-1}$ is the process covariance

[1] It was assumed that the data rate and delay spread in the environment was low enough so that the effect of delay spread was negligible. Previous field trials [5] have shown this to be the case.

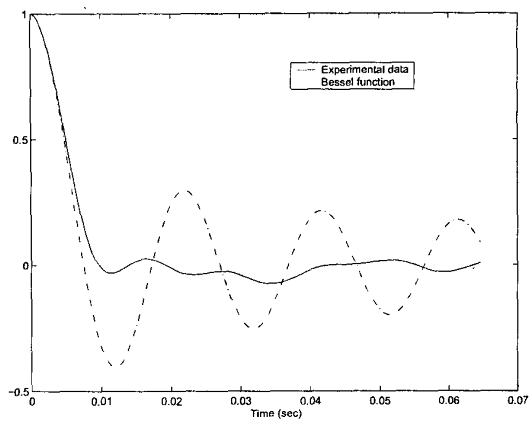

Fig. 1. Inphase fading autocorrelation function for case R (residential area).

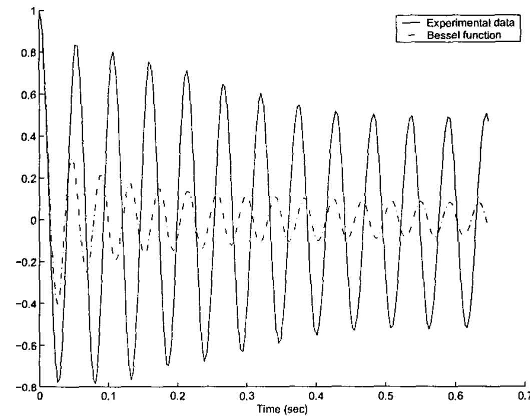

Fig. 2. Inphase fading autocorrelation function for case H (highway).

matrix:

$$\mathbf{D}^{-1} = [R(t_j - t_i)]_{k,k} \tag{3}$$

$R(\tau)$ is the process autocorrelation function. The noise multidimensional distribution has a similar form.

This model is called a Rayleigh fading, because its envelope $\alpha(t) = |c(t)|$ is Rayleigh distributed:

$$Pr\{\alpha(t) < a\} = 1 - exp(-0.5a^2/\mu) \tag{4}$$

If fading mean is non-zero, the fading is called Rician which accounts for the presence of a line-of-sight (LOS) component.

Different models of fading channels are based on different assumptions about the fading power spectral density $S(f)$ (or autocorrelation function $R(\tau)$). The Clarke's model ([1], [2]) assumes that

$$S(f) = \mu/\pi\sqrt{f_D^2 - f^2}, \quad R(\tau) = \mu J_0(2\pi f_D|\tau|) \tag{5}$$

where $J_0(\cdot)$ is the Bessel function of the first kind and f_D is the maximal Doppler frequency. The other models include rational functions ([9], [3], [10]), simple irrational functions ([9], [3]), and Gaussian PDF ([9]).

To validate the model, we compared the normalized autocorrelation function $J_0(2\pi f_D|\tau|)$ with that estimated from measured data for cases the R and H, respectively. Our results are depicted in Figures 1 and 2.

As we can see, the theoretical model does not fit well to the experimental data. We have observed also a significant correlation between the inphase and quadrature components as is seen in Figures 3 and 4.

III. Arma Model

It is well known that Gaussian stochastic processes can be modeled by filtering of white Gaussian noise $w(t)$:

$$c(t) = \int_{-\infty}^{\infty} h(\tau)w(t-\tau)d\tau \tag{6}$$

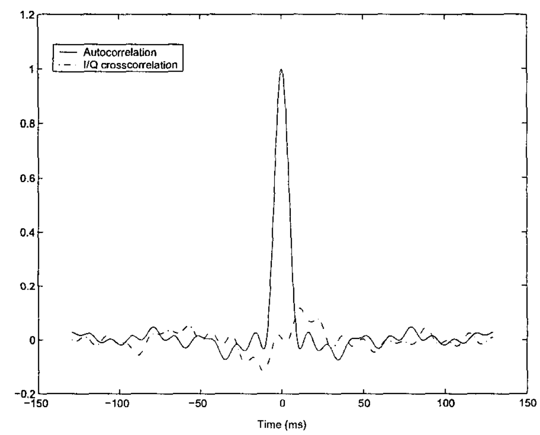

Fig. 3. Autocorrelation and crosscorrelation between inphase and quadrature fades for case R.

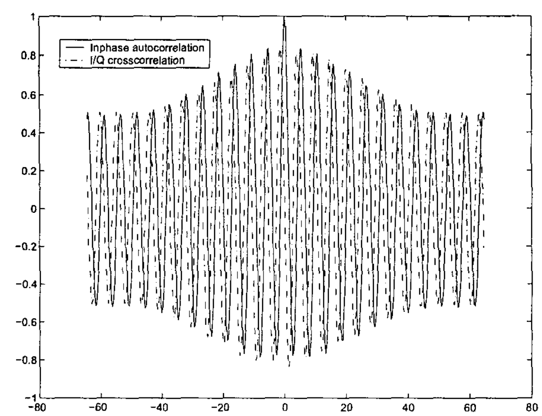

Fig. 4. Autocorrelation and crosscorrelation between inphase and quadrature fades for case H.

with the filter whose frequency response $H(jf)$ is found by the Wiener factorization of the power spectral density:

$$S(f) = H(jf)H^*(jf) \tag{7}$$

where $()^*$ denotes complex conjugation. This means that we can approximate fading using only moving average (MA) models (or FIR filter). The order of the MA model can be high. ARMA model (IIR filter) can give a more compact approximation.

The ARMA model is defined by the following equation

$$c_k = \sum_{i=1}^{p} h_i c_{k-i} + v_k, \quad v_k = \sum_{i=0}^{r} g_i e_{k-i} \tag{8}$$

where e_k is a noise (a sequence of independent identically distributed (i.i.d.) random variables). It is usually assumed that $g_0 = 1$ and the noise e_k represent zero mean Gaussian variables (discrete white Gaussian noise). To complete the process description, the initial conditions must be provided. We assume that these conditions correspond to the stationary state since we consider very long sequences.

It is clear from this description that the ARMA approximation of the fading is a special case of the Markov process whose state is defined by the vectors $\mathbf{c}_{k-p}^{k-1} = (c_{k-p}, c_{k-p+1}, ..., c_{k-1})$, $\mathbf{e}_{k-r}^{k-1} = (e_{k-r}, e_{k-q+1}, ..., e_{k-1})$. In the case of Gaussian noise, the ARMA is a Gauss-Markov process.

The model can be represented symbolically as

$$H(q)c_t = G(q)e_t \tag{9}$$

where $H(q)$ and $G(q)$ are the operator polynomials:

$$H(q) = \sum_{i=0}^{p} h_i q^{-i}, \quad G(q) = \sum_{i=0}^{r} g_i q^{-i} \tag{10}$$

q^{-i} is the shift operator: $q^{-i}c_t = c_{t-i}$.

The sequence c_k power spectrum is given by ([8])

$$S(f) = \sigma^2 \left| G(e^{2\pi jf})/H(e^{2\pi jf}) \right|^2 \tag{11}$$

where σ is the noise standard deviation. The process autocorrelation function has a matrix-geometric form and can be found analytically or by using the inverse Fourier transform of $S(f)$.

Most of the methods for fitting ARMA models to experimental data are based on minimizing some measure between the predicted and measured signals. This usually leads to fitting second order statistics. For Gaussian processes, this approach is optimal. Using the standard statistical methods, we fiited ARMA models with $r = 5$ and $p = 15$ to the experimental dat. The time unit for these models is 1/3094 sec. The models' autocorrelation functions and power spectral densities are compared with that of measured data in Figures 5,6,7, and 8.

As we can see, the power spectrum for the case R does not have a typical U-shape which is characteristic for the Clarke's model.

The PDFs of the residuals e_t PDF are compared with the theoretical Gaussian distributions in Figures 9 and 10.

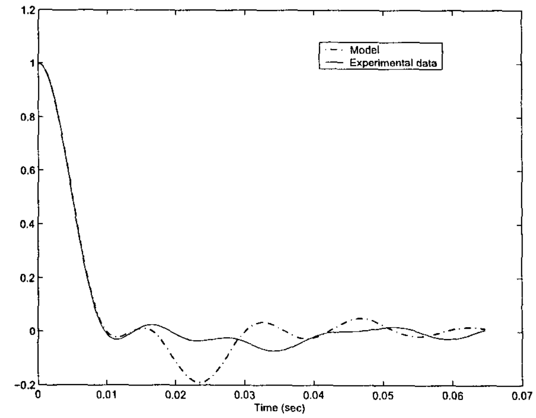

Fig. 5. Comparison of autocorrelation functions for the case R

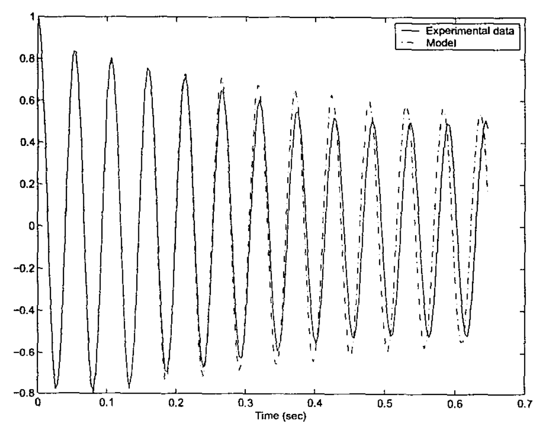

Fig. 6. Comparison of autocorrelation functions for the case H

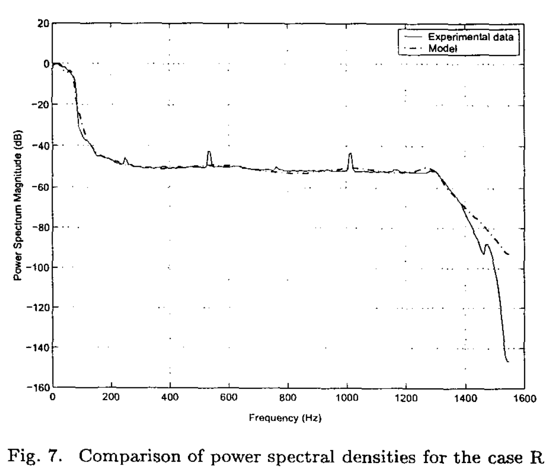

Fig. 7. Comparison of power spectral densities for the case R

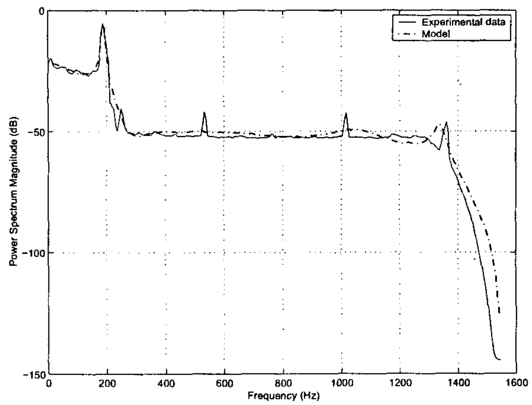

Fig. 8. Comparison of power spectral densities for the case H

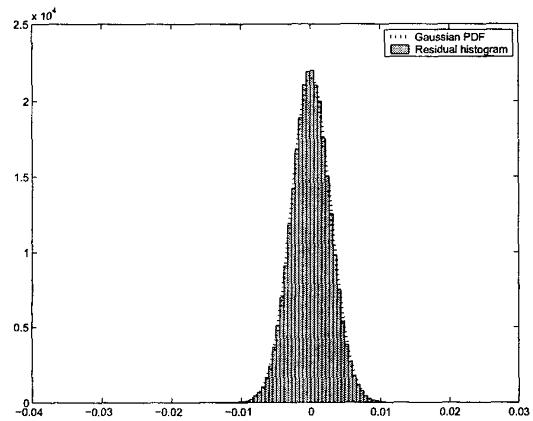

Fig. 9. Comparison of residual PDF with the Gaussian PDF for the case R

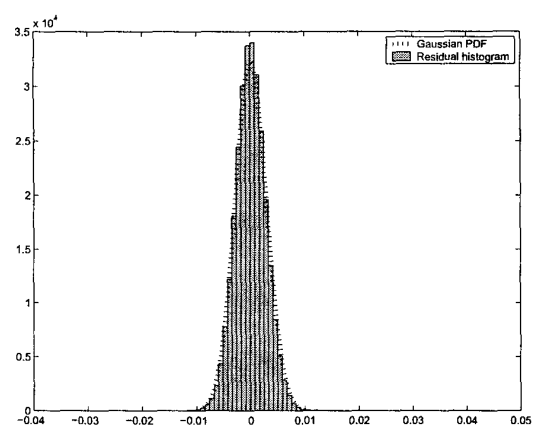

Fig. 10. Comparison of residual PDF with the Gaussian PDF for the case H

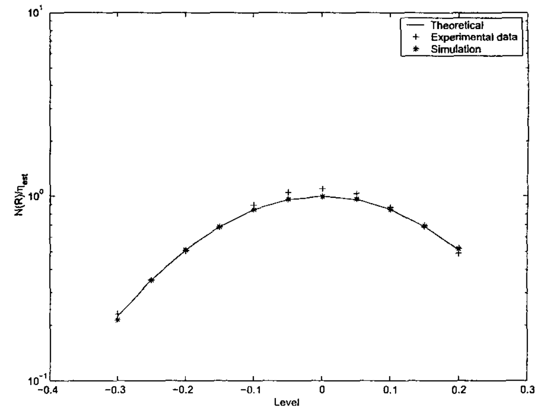

Fig. 11. LCR for the fade inphase component (case R).

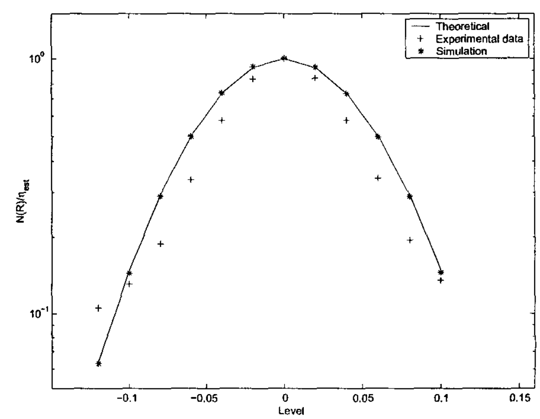

Fig. 12. LCR for the fade inphase component (case H).

IV. Model basic parameters

To see if the model agrees with experimental data, we compare the model's basic characteristics with that of measured data. Fade level-crossing rate (LCR) is an important characteristic of fading process. It can be used for estimating the Doppler frequency and, therefore, the vehicle velocity. For the Gaussian process with zero mean, the LCR for level x can be found from the following equation [9]

$$N(x) = \eta_x exp(-0.5\xi^2) \tag{12}$$

where $\xi = x/\sigma_x$,

$$\eta_x = \frac{1}{2\pi}\sqrt{-g''(0)/g(0)} \tag{13}$$

and $g(\tau)$ is the process autocorrelation function. Figures 11 and 12 compare the LCRs obtained using this equation with the experimental and simulated data. Simulated data was obtained using the ARMA models.

Duration of fades is another important parameter of the fading process. The average fade duration below level R

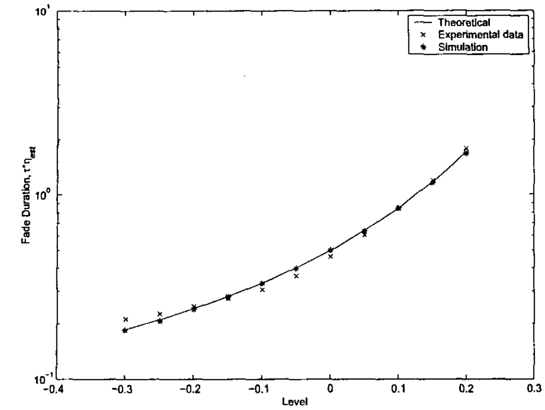

Fig. 13. Mean durations of fade inphase component (case R).

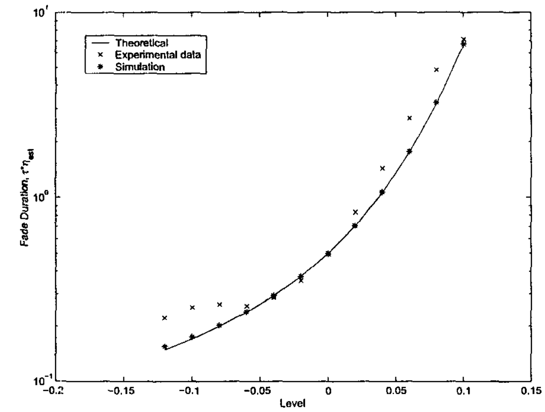

Fig. 14. Mean durations of fade inphase component (case H).

can be expressed as ([2], pg. 36)

$$\bar{\tau}(R) = P(r <= R)/N(R) \qquad (14)$$

where $P(r <= R)$ is the probability of fades below R. For the Gaussian process with zero mean

$$P(r <= R) = \frac{1}{\sqrt{2\pi}} \int_{-\infty}^{\xi} exp(-0.5u^2)du \qquad (15)$$

The results using this equation are compared with the experimental data in Figures 13 and 14.

V. Conclusion

In this paper, we demonstrate that fading in wireless communications can be modeled reasonably well by the ARMA models. This conclusion is based on comparison of measured and modeled characteristics of the fading process.

References

[1] R. H. Clarke, "A statistical theory of mobile radio reception," *Bell Syst. Tech. J.*, vol. 47, pp. 957-1000, 1968.

[2] W.C. Jakes, *Microwave Mobile Communications,* Wiley, 1974, New York.

[3] W.C.Y. Lee, em Mobile Communications Engineering, McGraw-Hill, 1982, New York.

[4] L. Ljung, *System Identification,* Prentice Hall, Upper Saddle River, NJ 1999. July 11, 2000.

[5] C. C. Martin, N. R. Sollenberger, and J. H. Winters, "Field test results of downlink smart antennas and power control for IS-136," *Proc. IEEE Veh. Technol. Conf.*, May 1999.

[6] C. C. Martin, J. H. Winters, and N. R. Sollenberger, "Multiple-input multiple-output (MIMO) radio channel measurements," *Proc. IEEE Veh. Technol. Conf.*, September 2000.

[7] J.G. Proakis, *Digital Communications,* McGraw-Hill, New York, 1989.

[8] L. Rabiner and B. Gold, *Theory and Applications of Digital Signal Processing,* Prentice Hall, Englewood Cliffs, New Jersey, 1975.

[9] S.O. Rice, "Distribution of the duration of fades in radio transmission: Gaussian noise model," *Bell Syst. Tech Journ.*, vol. 37, May 1958, pp. 581-635.

[10] F. Swarts and H.C. Ferreira, "Markov characterization of channels with soft decision outputs," *IEEE Trans. Commun.*, vol. 41, May 1993, pp. 678-682.

[11] W. Turin, *Digital Transmission Systems: Performance Analysis and Modeling*, McGraw-Hill, New York, 1998.

[12] W. Turin and R. van Nobelen, "Hidden Markov modeling of flat fading channels," *IEEE Journ. Sel. Areas. Comm.*, vol. 16, no. 9, 1998.